Extraction of signals of a phase transition from nuclear multifragmentation

Wolfgang Bauer
W. K. Kellogg Radiation Laboratory 106-38, California Institute of Technology, Pasadena, California 91125
(Received 8 February 1988)

We use a percolation model of nuclear fragmentation to study the possibility of observing a phase transition of nuclear matter in collisions of high-energy ($>$ 10 GeV) protons with heavy targets. It is shown that the model is able to reproduce experimental results for inclusive mass yields, while only using very simple physical assumptions. By employing event by event analysis of the moments of the mass distributions it is shown how to extract possible signals of a phase transition and information on its specific nature. Special attention is focused on the influence of the size of the fragmenting system on our ability to observe the phase transition.

I. INTRODUCTION

Do nuclei exhibit critical behavior in their multifragmentation after having been bombarded by high energy (>10 GeV) protons? This question has received renewed interest after the publication of the results of the Purdue group[1,2] who observed a power law

$$\sigma(A_F) \propto A_F^{-\lambda}, \quad A_F < A_T/3 \tag{1}$$

in the inclusive mass yield data for the reactions $p+\mathrm{Kr}$ and $p+\mathrm{Xe}$ at beam energies of 80 to 300 GeV. The value of the exponent λ was observed to be ≈ 2.6. Since the mass yield distribution of droplets condensing at the critical point in a van der Waals gas follows a similar power law

$$\sigma(m) \propto m^{-\tau} \tag{2}$$

with a value of $\frac{7}{3}$ for the critical exponent τ, the authors of Ref. 2 suggested that nuclear multifragmentation proceeds via a liquid-gas phase transition of nuclear matter.

Different theoretical fragmentation models based on a droplet description of the nucleus have been proposed,[3,4] and the liquid-gas phase transition has been studied extensively[5–7] in theoretical calculations.

Power laws in the mass distribution, however, are by no means unique to liquid-gas phase transitions. Hüfner and Mukhopadhyay[8] pointed out that power laws similar to Eq. (1) can be observed in other fragmenting systems as well. As examples they cite the mass distribution of asteroids in the solar system and the mass distribution of the debris of macroscopic basalt pellets being shot at each other.

Hüfner and his group have therefore proposed a so-called *minimum information model*.[9] This model only uses the law of charge conservation and the principle of maximum entropy for its predictions based on statistical calculations. It was later refined[10] and extended to include the law of total energy conservation.[11]

Another class of statistical models are the ones based on percolation theory, first introduced by our group[12,13] and by Campi and Desbois.[14] This class of models is now widely used[15–19] to describe experimental mass yield curves in high-energy fragmentation reactions.

In this paper we will apply percolation ideas to describe inclusive mass yield data in high-energy (>10 GeV) proton-induced fragmentation reactions of heavy targets. In Sec. II we will, therefore, briefly introduce the model used and show that using only very basic assumptions one is able to obtain good agreement with experimental data for the mass distribution of the fragments.

Section III will be used to study the influence of the finiteness of the fragmenting system on our ability to extract possible signatures of a phase transition. This point is of major concern, since it is not *a priori* clear exactly what signal of a phase transition to expect in systems of typically only ≈ 100 constituents, and how to extract information about the specific class of phase transitions from it.

Finally, in Sec. IV we will use our model predictions for an event-by-event moment analysis of the mass distribution similar to the one done by Campi.[16] In Sec. IV future experiments will be suggested, and predictions of their outcome will be made. It will be argued that it is possible to observe a phase transition of nuclear matter in fragmentation experiments well within the capabilities of present day accelerators and detector systems, and that this transition is one of the percolation type.

II. PERCOLATION MODEL OF NUCLEAR FRAGMENTATION

It is generally assumed that high-energy proton-induced fragmentation reactions proceed via a two-step process.[20] In the first step the incoming proton reacts with a tube of nucleons on its straight path through the target nucleus. This tube is emitted in the forward direction. In this first step a huge amount of energy is deposited in the spectator matter surrounding the tube. There is, however, only a small linear momentum transfer to the spectators, which can be inferred from moving source fits.[2] In the second step the highly excited spectator matter decays into fragments. We will use our percola-

tion model to describe this step.

Percolation models[21] are generally based on two ingredients: a description of the distribution of a set of points in a d-dimensional space and a criterion for deciding whether two given points are connected. Subsets of connected points are called *clusters*, and the study of these clusters constitutes percolation theory.

In general one distinguishes between bond and site percolation models. While Campi and Desbois[14] used a site percolation model, we have proposed a model based on bond percolation theory. The connection with bond percolation theory is established in our model as follows.

We represent the target nucleons by points occupying an approximately spherical volume on a simple cubic three-dimensional lattice in coordinate space. In general, it would be possible to use any lattice structure. However, for infinite systems the universality concept[22] tells us that the results obtained (critical exponents) are independent of the lattice structure. For the finite systems of interest in this paper this will be demonstrated in Sec. III.

The lattice spacing b can be computed approximately from the nuclear saturation density

$$b=\frac{1}{\rho_0^{1/3}}\approx 1.8 \text{ fm} . \tag{3}$$

The number of points used equals the number of target nucleons and is conserved during the calculation, therefore automatically fulfilling the conservation law of mass in the fragmentation process

$$\sum_{i=1}^{m} A_{\text{frag}}(i)=A_T , \tag{4}$$

where $A_{\text{frag}}(i)$ is the mass number of fragment i and m is the total multiplicity of all fragments.

The nucleons are connected to their $z=6$ nearest neighbors on the lattice via bonds representing the short-ranged nuclear interaction. These bonds are then broken with a probability p, which is the percolation parameter and depends linearly on the excitation energy per nucleon E^* of the target

$$p=\frac{E^*}{E_B}=\frac{E^*}{E_{\text{bond}}\cdot z/2} . \tag{5}$$

Here E_{bond} is the energy required to break one bond and E_B is the nuclear matter binding energy per nucleon (16 MeV).

There is no straightforward way of calculating the excitation energy E^* as a function of beam energy. Therefore, we will use p as an adjustable parameter which will be used to fit the experimental mass yield data. We can then use Eq. (5) to estimate the total excitation energy deposited in the target. We have to keep in mind, however, that the *Ansatz* of Eq. (5) can only be valid for excitation energies E^* which are smaller than the nuclear matter binding energy E_B. For higher excitation energies, which are for example reached in the participant matter in central heavy-ion collisions at Bevalac energies, Eq. (5) cannot be valid, because probability values greater than 1 would result.

It is interesting to note the similarity between the Bethe-Weizsäcker description of the nuclear binding energy and the result using our approach. Consider, for example, the Ag nucleus. Calculating the binding energy per nucleon using the volume and surface term only of the Bethe-Weizsäcker formula yields

$$E_b=15.75 \text{ MeV}-17.8 \text{ MeV}\times 108^{-1/3}\approx 12 \text{ MeV} . \tag{6}$$

Representing the Ag nucleus on our lattice requires ≈ 240 bonds, every one of which represents a binding energy of

$$E_{\text{bond}}=15.75 \text{ MeV}\times 2/z=5.25 \text{ MeV} .$$

Therefore, we obtain an effective binding energy per nucleon of

$$E_b=\frac{240E_{\text{bond}}}{108}\approx 11.7 \text{ MeV} \tag{7}$$

which is quite close to the value obtained above. We can therefore conclude that we are able to take approximate care of volume and surface effects in the binding energy by placing our nucleons on a lattice. In both approaches the same Coulomb energy has to be added to calculate the total binding energy.

Clearly, the breaking probability p of Eq. (5) has to be dependent on the impact parameter b of the proton. A physically sensible way of modeling this dependence without any adjustable parameter is to integrate over the nucleon density of the target along the path of the projectile

$$p(b)=\frac{p_0\int_{-\infty}^{+\infty}\rho[\mathbf{R}(b)]d\mathbf{R}}{\int_{-\infty}^{+\infty}\rho[\mathbf{R}(0)]d\mathbf{R}} . \tag{8}$$

For numerical calculations a standard Woods-Saxon parametrization of the density $\rho(\mathbf{r})$ is used. Thus p is a monotonically falling function of b and $p(0)=p_0$. This approach is motivated by the Glauber approximation and will be used to describe the impact parameter dependence of p. For a given b we will use a uniform breaking probability for the entire lattice corresponding to a thermalized system. We have used different spatial dependences of p, but did not obtain satisfactory results.

For a given $p(b)$ we generate a random number ζ_{ijk} between 0 and 1 for every bond B_{ijk} (where the indices correspond to the spatial location of the center of the bond on the lattice) and decide if the bond will be broken,

$$\zeta_{ijk}\begin{cases} >p \Longrightarrow B_{ijk} \text{ unbroken} \\ \leq p \Longrightarrow B_{ijk} \text{ broken.} \end{cases} \tag{9}$$

Then we use a cluster search algorithm described in Ref. 12 to find out which nucleons are still connected via bonds and identify these clusters with the fragments of the nuclear collision.

By summing over all impact parameters and using a large number of Monte Carlo events we are thus able to generate mass inclusive mass yield distributions that can be compared to experimental results

$$A_F = \frac{\int d^2b\, A_F[p(b)]}{\int d^2b} \ . \tag{10}$$

It should be mentioned here that the only adjustable parameter in our model is the value of the constant p_0 entering into Eq. (8). The histogram in Fig. 1 has been obtained using our model calculation with a value of $p_0 = 0.92$. The experimental data are taken from Ref. 23 and are represented by the circles. It is amazing that our simple model is able to nicely reproduce not only the right absolute normalization, but also the overall shape of the mass yield curve. While the agreement for small and large mass fragments is excellent, our calculations underpredict the data by a factor of 2 to 3 in the mass region between 40 and 90.

Using Eqs. (5) and (8) we can also estimate the total excitation energy deposited in the target. For a central collision of the proton with the Ag nucleus we obtain a total excitation energy of the spectator matter of

$$E^*_{\text{total}} = p_0 \cdot E_b \cdot A_T \approx 1600 \text{ MeV} \ , \tag{11}$$

where a value of $E_b = 15.75$ MeV was used.

We have mentioned before that the experimental data follow a power law given in Eq. (1). In an earlier paper we have shown[13] that for every constant p a percolation *Ansatz* will result in a power law for the low-to-medium mass fragments with a falloff constant λ which is a function of p and has a minimum of $\lambda = 2.18$ for $p = p_{\text{crit}} = 0.7$.

In inclusive experiments one is only able to measure fragment mass distributions that contain contributions from all impact parameters. Thus one is only able to measure an effective λ which is averaged over all impact parameters. This is also true for the inclusive results of our calculations displayed in Fig. 1. It is quite surprising that the inclusive data also follow a power law with an effective exponent λ. However, it turns out that we can extract a value of $\lambda = 2.6$ from our data using all fragment masses between 1 and 20 via linear regression with a correlation coefficient $r = 0.9995$. For other values of p_0 one obtains different values for λ, and p_0 was chosen to reproduce the experimental findings for λ from Ref. 2.

It is very interesting to look at different impact parameter intervals and analyze the fragment mass distributions from every interval separately. For Fig. 2 we therefore chose four different intervals in a way that

$$2\pi \int_{b_{\min}}^{b_{\max}} b\, db = \frac{\sigma_{\text{tot}}}{4} = \frac{\pi R_T^2}{4} \ . \tag{12}$$

In this way the absolute normalizations of the fragment spectra for all intervals are readily comparable.

The shapes of the mass yield curves in Fig. 2 agree with what one would intuitively expect. For small impact parameter b (central and most violent collisions) the target breaks up into small fragments. In the ring 2.85 fm $< b <$ 4.03 intermediate mass fragments up to mass $A_T/2$ are also produced. In the impact parameter interval between 4.03 and 4.94 fm we are able to produce essentially all fragment masses over the whole mass range. For large b (peripheral collisions), finally, we obtain typical spallation mass distributions: Only small fragments are broken off the target nucleus.

In every impact parameter interval it is possible to extract a separate exponent λ_i from our calculations. The values extracted from Fig. 2 are from top to bottom $\lambda_i = -3.42$, -2.30, -2.41, and -3.67. Therefore, it is clear that the exponent λ extracted from inclusive reac-

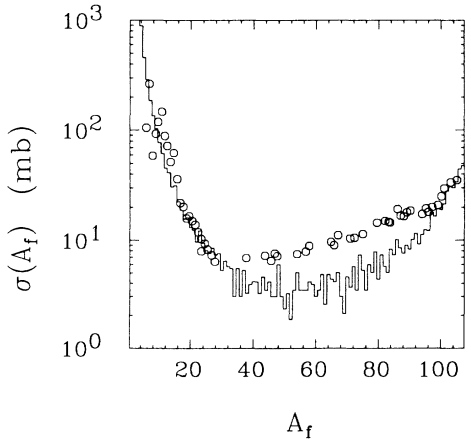

FIG. 1. Comparison of our calculations (histogram) for the mass yield curve to the experimental data (plot symbols) of Ref. 23 for the reaction p + Ag at 300-GeV beam energy.

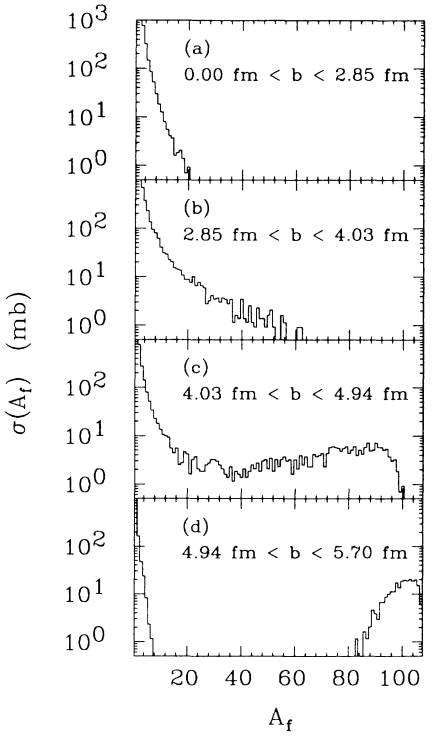

FIG. 2. Contributions from different impact parameter intervals to the theoretical curve shown in Fig. 1.

tions is by no means a unique constant, but varies with impact parameter.

We have already mentioned that the critical percolation probability for the system under consideration is $p_c=0.7$. Since $p(0)=0.92$ and $p(b)$ falls off radially to 0, there will be a certain impact parameter interval in which $p(b)\approx p_c$. The impact parameter at which this happens is included in the interval 2.85 fm <4.03 fm, as already indicated by the lowest value of λ_i extracted for this interval.

We conclude that we obtain overcritical events for central collisions and undercritical events for peripheral collisions. But there will be a certain impact parameter interval which produces critical events. Therefore, collisions of high-energy protons with heavy targets provide an ideal laboratory to scan across this phase transition. By looking at different impact parameters we can vary the excitation energy of the spectators without changing the beam energy. In addition, there is the phenomenon known as limiting fragmentation[24,25] which indicates that only a finite energy can be deposited into the spectator matter. Therefore, it is not even necessary to be very careful in choosing the beam energy, as long as it is above a value of ≈ 10 GeV.

III. FINITE-SIZE EFFECTS

Theories of phase transitions are generally formulated for practically infinite systems. We therefore have to address the question whether it is feasible to recover signals of a phase transition in systems with typically only 100 constituents. Our numerical studies will again concentrate on finite percolation systems.

In Fig. 3(a) we display the average multiplicity $\langle m \rangle$ of all fragments per lattice site as a function of our percolation parameter p. The solid line represents the result of our calculation on a simple cubic lattice with 108 lattice sites. The dashed line is the result for an infinite simple cubic lattice.[26] We can see that for $p=0.7$ the average total multiplicity per site is about twice as high for the finite system as compared to the infinite. Since this is the region we want to explore in studying the phase transition, it appears that this is a large discrepancy.

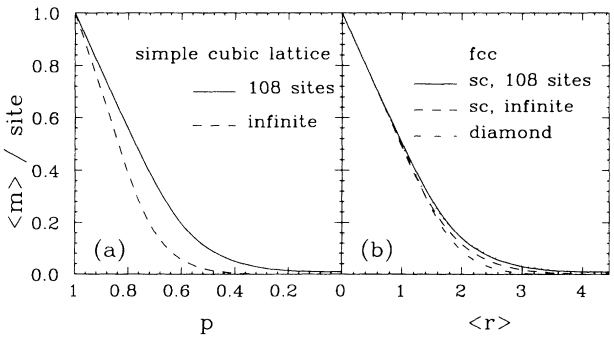

FIG. 3. (a) Comparison of the mean multiplicity per site as a function of p for an infinite simple cubic lattice and a finite simple cubic lattice of 108 sites. (b) Comparison of the mean multiplicity per site as a function of the mean coordination for the finite simple cubic lattice and three different infinite lattices.

Similar to treating the surface effects on the binding energy, we will try to incorporate finite-size effects on $\langle m \rangle$ per site by defining an average effective number of nearest neighbors on the finite lattice

$$z_{\text{eff}}=\frac{N_{\text{bonds}}}{N_{\text{nucleons}}} . \tag{13}$$

For our problem with 108 lattice sites representing the Ag nucleus we obtain $z_{\text{eff}}\approx 4.44$.

To eliminate most of the effects of the lattice structure one usually defines the mean coordination

$$\langle r \rangle = z\cdot(1-p) \tag{14}$$

in percolation theory.[27] In Fig. 3(b) we plot again $\langle m \rangle$ per site, but now as a function of $\langle r \rangle$. The dotted line represents the face-centered cubic lattice ($z=12$), the dashed-dotted line stands for the diamond structure ($z=4$), and the dashed line is the result for a simple cubic lattice ($z=6$). Using the value z_{eff} obtained above we can compare the result of the finite system (solid line) with the infinite lattices. It is apparent that our results are practically independent of the lattice structure used, and that it is also possible to include most finite-size effects in the way just described.

In the next section we will use the moments of the cluster mass distribution to analyze our data. Therefore, it is important to investigate if and how the finiteness of the system affects a moment analysis. We define the moments of the mass yield distribution

$$M_k(p)=\sum_{A_f} (A_f)^k\cdot N_{A_f}(p) , \tag{15}$$

where N_{A_f} is the number of fragments with mass A_f obtained for a given p

$$N_{A_f}(p)=\frac{1}{N_{\text{tot}}}\sum_{i=1}^{N_{\text{tot}}} n_i(A_f,p) . \tag{16}$$

Here N_{tot} is the total number of events used in the average (we typically used $N_{\text{tot}}=1000$) and $n_i(A_f,p)$ is the number of times a cluster of mass A_f is obtained in the event i.

In standard percolation theory the A_f sum in Eq. (15) is carried out over all finite-size clusters. The infinite percolation cluster is excluded. In our finite percolation model the obvious upper limit seems to be the target mass.

In Fig. 4(a) we display the ratio M_2/M_1 as a function of p with the sum of Eq. (15) terminating at A_T. Even though percolation theory tells us that M_2/M_1 should diverge for $p=p_c$, we cannot see this in the figure. The ratio decreases monotonically with p from 108 ($=A_T$) to 1.

In finite systems it is therefore not enough to sum only over all finite clusters, but we have to truncate the sum in Eq. (15) before the clusters reach the size of the system (in this case 108 sites). In part (b) of Fig. 4 we have introduced an upper cut in the summation for Eq. (15). The

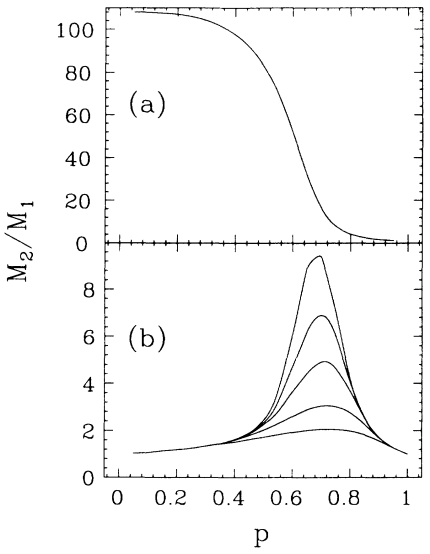

FIG. 4. (a) Value of M_2/M_1 as a function of p using no cutoff in the fragment mass. (b) M_2/M_1 as a function of p using cutoff mass values of (from top to bottom) 40, 30, 20, 10, and 5.

curves represent from bottom to top the results for cutoff masses $m_{\text{cut}}=5$, 10, 20, 30, and 40. We can now see an indication of the expected divergence around $p_c=0.7$. We found that for practical applications it it not useful to work with cutoff masses $m_{\text{cut}} > A_T/2$, because the influence of the "infinite" cluster will be visible in the moments of the fragment mass distribution. This is of special importance in cases where fission of the target occurs. The large values of the moments for these noncritical events would otherwise contaminate the results obtained from our analysis.

IV. EVENT-BY-EVENT ANALYSIS

Up to now we have displayed the moments of the cluster size distribution as a function of the breaking probability p which is not a direct experimental observable. This is due to the fact that in the definition of the moments in Eq. (15) we used distributions N_{A_f} which are averages over many events for one constant value of p. To avoid this difficulty Campi[16] proposed an event-by-event analysis of the momenta of the cluster size distribution. Now every event i produces a value $M_k^i(p)$ which is defined as

$$M_k^i(p)=\sum_{A_f}(A_f)^k\cdot n_i(A_f,p)\ . \tag{17}$$

The advantage of this technique is that $M_k^i(p)$ can be computed without a knowledge of p for this event. One can therefore plot values of different moments versus the multiplicity or versus each other without having to have prior knowledge of p in every event.

With this event-by-event technique it is possible to obtain valuable insight into the question whether a phase transition occurs in nucleon-nucleus collisions. In addition, one should be able to make statements concerning the specific nature of the phase transition, as we will show in the following.

In Fig. 5 we investigate the question what the signature of the occurrence of a phase transition in our finite system is. For Fig. 5(a) we simulated 5000 events using our model and a value of $p_0=0.6$. Therefore, all values of p used in generating Fig. 5(a) are below the critical value of 0.7. We have computed the values of M_2 and $M_0=$multiplicity, and every point represents one event simulation. A cutoff mass of $m_{\text{cut}}=30$ was used. In part (b) of Fig. 5 we used the same procedure, but this time using a value of $p_0=0.92$ which was also used to generate the calculations for Fig. 1. The target mass was again taken to be 108. While part (a) only contains undercritical events, part (b) contains undercritical as well as critical and overcritical events.

We can see a clear difference in the two results. First of all, we note that in Fig. 5(b) much higher multiplicities are reached. This is not too surprising, since we know that the total multiplicity is monotonically increasing with p. But more important, we can see that M_2 reaches a maximum for intermediate values of the multiplicity and then slowly falls off again. This has to be interpreted as the signal that the event spectrum contains critical and overcritical events as well as the undercritical ones.

Since we were able to reproduce the features of the inclusive mass yield curve for the $p+$Ag reaction in Fig. 1 with the value of $p=0.92$, we predict that a similar analysis of the experimental data should show a result such as Fig. 5(b). This then could be interpreted as a signature that a phase transition has occurred. Therefore, it would be strongly desirable to perform this kind of fragmentation experiment using 4π mass detectors.

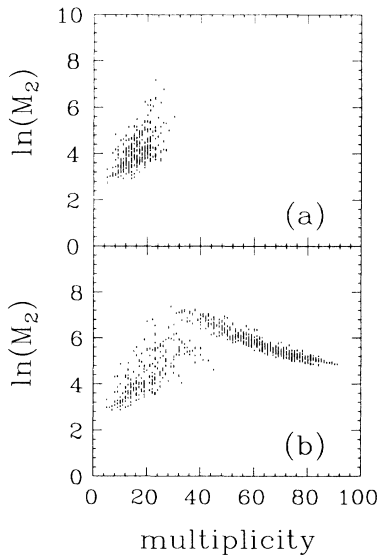

FIG. 5. Event-by-event spectrum of M_2 vs the total multiplicity in a theoretical simulation containing only undercritical (a) and both undercritical as well as critical and overcritical (b) events. In both cases a target mass of 108 and a cutoff mass of 30 were used.

It is worth mentioning that the events with the highest multiplicities are not the ones with the highest values of M_2, the critical events. Therefore, one should not trigger the experiments on the highest values of the multiplicity reached in these reactions. It is more desirable from our point of view not to use any trigger condition and plot the data in the way done in Fig. 5 which will then determine if the data contain events in the critical region.

We should point out that a similar analysis has been done by Campi[16] analyzing the data of Waddington and Freier.[28] However, he plots M_2/M_1 versus the mass of the largest fragment. It appears to us that our approach is more robust with respect to experimental detection uncertainties. In these target fragmentation reactions the heaviest fragment usually has only a very small velocity in the laboratory frame and is hard to detect. Using our method one has only to detect the light fragments up to a certain cutoff mass. For the multiplicity it is not even very crucial if one of these fragments is not detected, since the value of the total multiplicity would change only by 1 which is only a small change and does not change the result qualitatively.

The main question of interest is now whether we are able to recover the correct values of the critical exponents for the phase transition from our finite systems. Scaling theory[21] relates the values of the critical exponents σ and τ to the moments M_k of the mass distribution via

$$M_k \propto |p-p_c|^{-(1+k-\tau)/\sigma} . \tag{18}$$

In the derivation of Eq. (18) the scaling assumption

$$N_{A_f}(p) \propto A_f^{-\tau} \cdot f[A_f^{\sigma} \cdot (p-p_c)] \tag{19}$$

was used which is a generalization of Fischer's scaling function[5]

$$N_{A_f}(p) \propto A_f^{-\tau} \cdot \exp[\text{const} \cdot A_f^{\sigma} \cdot (p-p_c)] . \tag{20}$$

The values of σ and τ entering into Eq. (18) are characteristic for the specific class of phase transition. For a transition of the three-dimensional (3D) percolation type we expect $\tau=2.2$ and $\sigma=0.45$. For a liquid-gas phase transition in mean field approximation one obtains a value of $\tau=\frac{7}{3}$ and $\sigma=\frac{2}{3}$. Using the Wilson renormalization group techniques[29] one obtains a values of $\tau=2.21$ and $\sigma=0.63$.

In Fig. 6 we show a plot of M_2 versus M_3 using the event-by-event technique. Since both moments diverge for infinite systems and we know that remnants of this divergence are present in finite systems (as shown in Fig. 4), M_2 and M_3 assume their maximum around the critical value of p. In order to find out if we can recover the critical exponents in finite systems, we have to extract them graphically and compare the exact values as obtained using Eq. (18).

Using this equation we see that around the critical point the points (M_3,M_2) should fall on a straight line in a doubly logarithmic plot. The slope of this line is given by

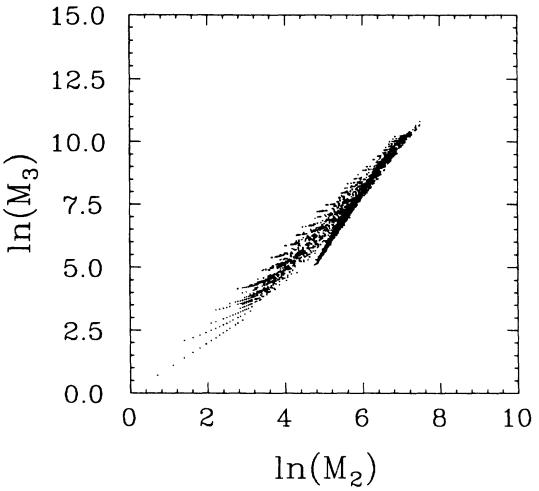

FIG. 6. Event-by-event spectrum of M_3 vs M_2 in a doubly logarithmic plot. A target mass of 108 and a cutoff mass of 30 were used, and a sample of 5000 events was generated in the theoretical simulation.

$$\begin{aligned}\mu &= \frac{\Delta \ln M_3}{\Delta \ln M_2} \\ &= \frac{(-1-3+\tau)/\sigma \cdot \Delta \ln |p-p_c|}{(-1-2+\tau)/\sigma \cdot \Delta \ln |p-p_c|} \\ &= \frac{\tau-4}{\tau-3} \\ &= 2.25 ,\end{aligned} \tag{21}$$

where in the last line the percolation value of $\tau=2.2$ was used.

From the slope of the highest values of M_3 and M_2 in Fig. 6 we graphically extract a value of $\mu=2.21\pm0.1$ which is in reasonable agreement with the theoretical value for the infinite system.

For comparison, we mention that the theoretical value for μ would be 2.5 in a liquid-gas–type phase transition in mean-field approximation, and that one obtains $\mu=3.0$ for percolation on a Bethe lattice. Therefore, the slope μ is characteristic for the specific nature of the phase transition. In addition, as we have shown, one is able to recover the proper value of the critical exponents even in finite systems of only ≈ 100 constituents. It is therefore worthwhile to perform a similar analysis of experimental exclusive mass yield data. As already mentioned, Campi[16] has done such an analysis to a very small sample of data points (about 400 events) and finds that the value of μ extracted from the data is 2.22 ± 0.1, from which he concludes that nuclei might indeed breakup like percolation clusters. However, as mentioned before, the value of $\tau=2.21$ obtained from the Wilson renormalization-group approach is very close to the percolation value, and thus it will also yield a value of $\mu \approx 2.25$.

V. DISCUSSION

We have forwarded a statistical model of multifragmentation for high-energy proton induced reactions. The model is not meant to deliver a self-consistent description of the whole fragmentation process in the way that approaches based on nuclear transport theory[30–32] attempt to do. However, it is very useful in modeling the statistical decay of the highly excited nuclear matter and enables us to undertake studies of the features of the reaction without a large usage of computer time.

Using only one free parameter and simple geometrical considerations we are able to reproduce experimental mass yield curves with a surprising degree of accuracy in high-energy proton induced multifragmentation reactions of heavy targets. Even though nuclei are not lattices and one should be very careful with applying such a concept to nuclear physics, we think we have shown the usefulness of percolation ideas in nuclear fragmentation.

From our analysis we extract that the observed power law in the low-to-medium mass fragments is not a characteristic feature of the specific reaction, but is rather an averaged quantity with different contributions arising from different excitation energies for different impact-parameter intervals.

We predict that the inclusive data contain critical and overcritical events as well as undercritical ones, or in other words, that is is possible to detect signals of a phase transition of nuclear matter in the reactions under consideration. To do this, experiments using 4π fragment mass detectors and an analysis similar to the one done above are needed. It should then be possible to not only detect traces of a phase transition, but also make statements about the specific nature of it.

Finally we should point out that similar excitation energies such as the energies deposited in the spectator matter in the reactions discussed above could also be obtained in central intermediate energy (40–100 MeV/nucleon) heavy-ion reactions for the participant region. This might offer an additional chance to observe the phase transition, provided that a stage of thermalization is reached in these reactions. The main difference in heavy-ion collisions would be that the decaying nuclear system starts out from a compressed initial state at roughly twice nuclear matter density instead of normal nuclear matter density as in the case of the proton-induced reactions.

ACKNOWLEDGMENTS

The author would like to acknowledge several helpful discussions with Professor U. Mosel and Professor M. F. Thorpe during the course of this study and Professor S. E. Koonin for a critical reading of the manuscript. This work was supported by National Science Foundation Grants Nos. PHY85-05682 and PHY86-04197.

[1] J. E. Finn, S. Agarwal, A. Bujak, J. Chuang, L. J. Gutay, A. S. Hirsch, R. W. Minich, N. T. Porile, R. P. Scharenberg, B. C. Stringfellow, and F. Turkot, Phys. Rev. Lett. **49**, 1321 (1982).

[2] A. S. Hirsch, A. Bujak, J. E. Finn, L. J. Gutay, R. W. Minich, N. T. Porile, R. P. Scharenberg, B. C. Stringfellow, and F. Turkot, Phys. Rev. C **29**, 508 (1984).

[3] J. Randrup and S. E. Koonin, Nucl. Phys. **A356**, 223 (1981).

[4] D. H. E. Gross, Nucl. Phys. **A428**, 313c (1984).

[5] M. E. Fischer, Physics **3**, 255 (1967).

[6] A. L. Goodman, J. I. Kapusta, and A. Z. Mekjian, Phys. Rev. C **30**, 851 (1984).

[7] A. D. Panagioutou, M. W. Curtin, H. Toki, D. K. Scott, and P. J. Siemens, Phys. Rev. Lett. **52**, 496 (1984).

[8] J. Hüfner and D. Mukhopadhyay, Phys. Lett. **173B**, 373 (1986).

[9] J. Aichelin, J. Hüfner, and R. Ibarra, Phys. Rev. C **30**, 107 (1984).

[10] L. G. Sobotka and L. G. Moretto, Phys. Rev. C **31**, 668 (1985).

[11] L. P. Csernai and J. I. Kapusta, Phys. Rep. **131**, 223 (1986). Y. Shibata and S. Fujita, Phys. Lett. **172B**, 283 (1986).

[12] W. Bauer, D. R. Dean, U. Mosel, and U. Post, Phys. Lett. **150B**, 53 (1985).

[13] W. Bauer, U. Post, D. R. Dean, and U. Mosel, Nucl. Phys. **A452**, 699 (1986).

[14] X. Campi and J. Desbois, in *Proceedings of the 23rd Bormio Conference* (Ricerca Scientifica ed Educatione Permanente, Milano, 1985), p. 497.

[15] T. S. Biro, J. Knoll, and J. Richert, Nucl. Phys. **A459**, 692 (1986).

[16] X. Campi, J. Phys. A **19**, L917 (1986).

[17] J. Nemeth, M. Barranco, J. Desbois, and C. Ngô, Z. Phys. A **325**, 347 (1986).

[18] J. Desbois, Nucl. Phys. **A466**, 724 (1987).

[19] C. Cerruti, J. Desbois, R. Boisgard, C. Ngô, J. Natowitz, and J. Nemeth, Nucl. Phys. **A476**, 74 (1988).

[20] R. Serber, Phys. Rev. **72**, 1114 (1947).

[21] D. Stauffer, Phys. Rep. **54**, 1 (1979).

[22] *Phase Transitions and Critical Phenomena,* edited by C. Domb and M. S. Green (Academic, London, 1972–1976), Vols. 1–6.

[23] A. Bujak, J. E. Finn, L. J. Gutay, A. S. Hirsch, R. M. Minich, G. Paderewski, N. T. Porile, R. P. Scharenberg, B. C. Stringfellow, and F. Turkot, Phys. Rev. C **32**, 620 (1985).

[24] S. B. Kaufmann und E. P. Steinberg, Phys. Rev. C **22**, 167 (1980).

[25] J. Hüfner, Phys. Rep. **125**, 131 (1985).

[26] The results for the infinite percolation systems were communicated to me by Prof. M. F. Thorpe and W. Xia.

[27] M. F. Thorpe, J. Non-Cryst. Solids **57**, 355 (1983).

[28] C. J. Waddington and P. S. Freier, Phys. Rev. C **31**, 888 (1985).

[29] K. G. Wilson, Phys. Rev. B **4**, 3174 (1971); **4**, 3184 (1971).

[30] J. Aichelin and H. Stöcker, Phys. Lett. **176B**, 14 (1986).

[31] G. E. Beavais, D. H. Boal, and J. K. C. Wong, Phys. Rev. C **35**, 545 (1987).

[32] W. Bauer, G. F. Bertsch, and S. DasGupta, Phys. Rev. Lett. **58**, 863 (1987).